Hindawi Publishing Corporation
Indian Journal of Materials Science
Volume 2014, Article ID 459674, 9 pages
http://dx.doi.org/10.1155/2014/459674

*Research Article*

# Adsorbent Ability of Treated *Peganum harmala-L* Seeds for the Removal of Ni (II) from Aqueous Solutions: Kinetic, Equilibrium and Thermodynamic Studies

**Maryam Ghasemi,[1] Nahid Ghasemi,[1,2] and Javad Azimi-Amin[3]**

[1] *Department of Chemistry, Science Faculty, Arak Branch, Islamic Azad University, P.O. Box 38135-567, Arak, Iran*
[2] *Process Systems Engineering Center (PROSPECT), Faculty of Chemical Engineering, Universiti Teknologi Malaysia (UTM), P.O. Box 81310 Skudai, Johor, Malaysia*
[3] *Department of Agriculture, University of Mehrgan, P.O. Box 37816-54363, Mahalat, Iran*

Correspondence should be addressed to Maryam Ghasemi; maryam_ghasemi6282@yahoo.com
and Nahid Ghasemi; n-ghasemi@iau-arak.ac.ir

Received 27 December 2013; Accepted 5 February 2014; Published 27 March 2014

Academic Editors: R. K. Dey, S. K. Kansal, and S. S. Sharma



The main goal of this study was to evaluate the performance of new adsorbent, treated *Peganum harmala-L* seeds (TPHS), for the removal of Ni (II) from aqueous solution. Batch experiments were performed as a function of various experimental parameters. The adsorption studies included both equilibrium adsorption isotherms and kinetics. Equilibrium data fitted very well with the Langmuir isotherm model. Maximum adsorption capacity was determined 91.74 mg/g at pH 7. Kinetics studies showed better applicability for pseudo-second-order model for both adsorbents. The negative value of $\Delta G^{\circ}$ confirmed the feasibility and spontaneity of TPHS for Ni (II) adsorption.

## 1. Introduction

Removal of heavy metals from wastewaters and industrial wastes has become a very important environmental issue. Nickel salts are commonly used in silver refineries, electroplating, zinc base casting, storage battery industries, printing, and in the production of some alloys that discharge significant amount of nickel in various forms to the environment. At higher concentrations, Ni (II) causes lung, nose, and bone cancer; headache; dizziness; nausea and vomiting; chest pain; tightness of the chest; dry cough and shortness of breath; rapid respiration; cyanosis; and extreme weakness. Hence, it is essential to remove Ni (II) from industrial wastewaters before it is discharged into natural water sources [1]. Adsorption is considered as effective, efficient, and economic method for water purification [2].

Since the performance of an adsorptive separation is directly dependent on the quality and cost effectiveness of the adsorbent, the last decade has seen a continuous improvement in the development of effective noble adsorbents in the form of activated carbons [3], zeolites [4], clay minerals [5], chitosan [6], lignocelluloses [7], natural inorganic minerals [8], and so forth. Adsorption onto activated carbon (AC) has proven to be one of the most effective and reliable physicochemical treatment methodologies. AC from cheap and readily available sources has been successively employed for removal of heavy metals [9]. There is only limited research on the preparation of activated carbons or modified natural adsorbent using *Peganum harmala-L* and its application for removing nickel from wastewaters. *Peganum harmala*, commonly called Esfand, Wild rue, Syrian rue, African rue, is a plant of the family Nitrariaceae. This plant is native from the eastern Iranian region west to India. *Peganum harmala-L* is abundant and inexpensive in Iran. However, microorganism-based and other biomasses often need to be prepared before application as biosorbent of metal

ions. This would increase the cost of the overall wastewater treatment process. Nickel was selected as adsorbate because its compounds have applications in many industrial processes such as nonferrous metal, mineral processing, paint formulation, electroplating, batteries manufacturing, forging, porcelain enameling, and copper sulphate. The chronic toxicity of nickel to humans and the environment has been well documented. High concentration of nickel causes cancer of lung, nose, and bone [10].

This work investigates the potential of treated *Peganum harmala-L* seeds in the removal of nickel ions from aqueous solutions. Batch studies were conducted using synthetic Ni ions solution to assess the adsorption kinetic, isotherm, and thermodynamics models. The structure of raw and treated *Peganum harmala-L* was characterized by FTIR and SEM analyses. A series of tests such as pH, adsorbent dosage, contact time of reaction and initial concentration of solution and temperature were done to study their effects on the Ni ion adsorption onto treated *Peganum harmala-L* seeds.

## 2. Adsorption Experiments

*2.1. Preparation of Treated Peganum Harmala-L Seeds.* *Peganum harmala-L* seeds were obtained from Khomein (located in the south of Markazi province) in Iran. Row seeds were air-dried, crushed, and impregnated with diluted $H_2SO_4$ (3 : 1). Then the materials were treated in a hot air oven at 80°C for 24 h. The carbonized material was washed with distilled water and then soaked in 1% $NaHCO_3$ solution to remove any remaining acid. It was washed with distilled water until the pH of the TPHS reached 6.5, dried at 105°C, and sieved to the particle size smaller than 0.125 mm.

*2.2. Preparation of Ni (II) Solutions.* The Ni ion concentration in the solutions was determined by Atomic Absorption Spectrometer (model AA 680 made of SHIMADZU). Before the analysis, the samples were diluted to the concentration of less than 100 ppm Ni (II) with distilled water.

The pH was measured via the Metrohm 827 made of Swiss pH meter. All chemicals were reagent grade and used without further purification.

Synthetic stock solution of 1000 mg/L of Ni was prepared by dissolving analytical grade $Ni(NO_3)_2{\cdot}6H_2O$ in double distilled water. Working solutions of the desired concentration were then prepared by successive dilution. All solutions were made using deionized distilled water.

*2.3. Batch Adsorption Experiments.* Batch experiments were conducted in order to study the effect of important parameters like pH, adsorbent dose, contact time, and initial ion concentration on the adsorptive removal of Ni ion using TPHS. The batch adsorption experiments, 10 mL solution of Ni (II) of initial concentration (100 mg/L), were contacted with 10 mg TPHS. The contents were placed in a stirrer and quietly shacked at 150 rpm. After shaking, the solution was filtered, and then remaining Ni concentration was analyzed. The effects of pH (2–10), contact time (5–90 min), the adsorbent dosage (1.0–15.0 mg), ion concentration (0.1–500 mg/L), and temperature (288–318 K) were tested. The amount of adsorbed Ni (II) at equilibrium ($q_e$) and Ni (II) removal efficiency (%$R$) were calculated from the following equations:

$$q_e = \frac{V}{M}\left(C_o - C_e\right), \qquad \%R = \frac{C_o - C_e}{C_o} \times 100, \tag{1}$$

where $C_e$ and $C_o$ are the final and initial concentrations of Ni (II) (mg/L), respectively, $V$ is the volume of Ni (II) solution ($L$), and $M$ is the mass of TPHS sample which is used in experiment (g).

*2.4. SEM Analysis and FTIR Spectroscopy.* The characterization of surface structure of the untreated and treated adsorbent was done using Scanning Electron Microscopy. To determine the functional groups involved in the metal adsorption process, the untreated and treated adsorbents were analyzed using a Fourier Transform Infrared Spectrometer (Bruker CO. Tensor 27, Germany) in the range of 400–4000 $cm^{-1}$.

*2.5. Adsorption Kinetic.* Adsorption rate constants for Ni (II) were calculated by using pseudo-first-order [11], pseudo-second-order [12], and intraparticle [13] models.

*2.5.1. Pseudo-First-Order and Pseudo-Second-Order Kinetic Models.* The pseudo-first-order equation is given by the Lagergren and presented in (2);

$$q_t = q_e\left[1 - \exp\left(-k_1 t\right)\right]. \tag{2}$$

The equation can be expressed in a linear form as follows:

$$\ln\left(q_e - q_t\right) = \ln q_e - k_1 t, \tag{3}$$

where $q_t$ (mg/g) is the amount of Ni (II) adsorbed at time $t$ (min), $q_e$ (mg/g) is the amount of the Ni (II) adsorbed on the adsorbent at time under equilibrium conditions, and $k_1$ is the pseudo-first-order rate constant (1/min). The rate constant $k_1$ (1/min) was calculated from the slope by plotting $\ln(q_e - q_t)$ versus $t$ for nickel.

The pseudo-second-order model is given by Ho and Mckay and shown in

$$q_t = \frac{t k_2 q_e^2}{1 + t k_2 q_e} \tag{4}$$

which can be rewritten as

$$\frac{t}{q_t} = \frac{1}{k_2 q_e^2} + \frac{t}{q_e}, \tag{5}$$

where $k_2$ is the pseudo-second order rate constant (mg/g·min). The linear plot of $t/q_t$ against $t$ was made in order to calculate the second-order rate constant $k_2$ and equilibrium adsorption capacity $q_e$ from slope and intercept, respectively.

*2.5.2. Intraparticle Model.* Weber and Moris proposed the kinetic model for the diffusion controlled sorption process. The intraparticle diffusion equation is given by (6), where $k_d$ is the intraparticle rate constant (mg/g·min$^{0.5}$), as follows:

$$q_t = k_d t^{1/2} + C. \tag{6}$$

The slope of the plot of $q_t$ against $t^{0.5}$ leads to the value of the intraparticle rate constant and $C$ (mg/g) is a constant that gives an idea about the thickness of the boundary layer; that is, the larger value of $C$, the greater the boundary layer effect.

*2.6. Adsorption Isotherms.* In order to describe the adsorption isotherm, three important isotherms were selected in this study, the Langmuir isotherm (7), the Freundlich isotherms (9), and the Temkin isotherm (10).

The Langmuir isotherm [14] is as follows:

$$\frac{C_e}{q_e} = \frac{C_e}{q_m} + \frac{1}{q_m K_L}, \tag{7}$$

where $C_e$ is the equilibrium concentration (mg/L), $q_e$ is the amount adsorbed onto the adsorbent (mg/g), $q_m$ is $q_e$ for complete monolayer adsorption capacity (mg/g), and $K_L$ is the equilibrium adsorption constant (L/mg).

The essential features of the Langmuir isotherm can be expressed in terms of dimensionless constant separation factor $R_L$ [15]:

$$R_L = \frac{1}{1 + K_L C_o}, \tag{8}$$

where $C_o$ (mg/L) is initial concentration of adsorbate and $K_L$ is the Langmuir constant (L/mg). There are four probabilities for the $R_L$ value: for favorable adsorption, $0 < R_L < 1$; for unfavorable adsorption, $R_L > 1$; for linear adsorption, $R_L = 1$; and for irreversible adsorption, $R_L = 0$.

The Freundlich isotherm [16] is as follows:

$$\ln q_e = \frac{1}{n} \ln C_e + \ln K_F, \tag{9}$$

where $K_F$ (mg/g) is the Freundlich adsorption constant and $1/n$ is a measure of the adsorption intensity. Values range $1 < n < 10$ indicate adsorption is considered favorable.

The Temkin isotherm [17] is as follows:

$$q_e = M_T \ln K_T + M_T \ln C_e, \tag{10}$$

$$M_T = \frac{RT}{b}, \tag{11}$$

where $K_T$ (L/mol) is the binding equilibrium constant corresponding to the maximum binding energy, $M_T$ (mol/g) is related to the heat of adsorption, $R$ (8.314 J/mol·K) is the universal gas constant, $T$ (K) is the absolute temperature (K), and $b$ is the constant related to the heat of adsorption.

*2.7. Adsorption Thermodynamics.* Thermodynamic parameters, the change in Gibbs free energy ($\Delta G^\circ$), enthalpy ($\Delta H^\circ$), and entropy change ($\Delta S^\circ$), in order to determine the feasibility of adsorption, were calculated using the following equations:

$$\Delta G^\circ = -RT \ln K,$$
$$\ln K = -\frac{\Delta H^\circ}{RT} + \frac{\Delta S^\circ}{R}, \tag{12}$$

where $K = q_e/C_e$, $q_e$ is the amount of ion adsorbed (mg/g), $C_e$ is the equilibrium concentration (mg/L), $T$ is temperature (K), and $R$ is the gas constant (8.314 J/mol·K) [18]. $\Delta H^\circ$ and $\Delta S^\circ$ values were calculated from the slope and intercept of the plot of $\ln K$ versus $1/T$.

## 3. Results and Discussion

*3.1. Surface Characterization.* Figures 1(a) and 1(b) show SEM images of raw *Peganum harmala-L* and treated *Peganum harmala-L*, respectively. Figures 2(a) and 2(b) show FTIR spectra of raw and treated *Peganum harmala-L*. As it can be seen from Figures 1(a) and 1(b), the surface of adsorbent before pre-treated treated has homogenous surface with regular pores that covers the entire surface. After treating, it has deep pores and irregular and heterogeneous surface which showed a good possibility for adsorption of Ni ions to be adsorbed into these pores. Both spectra have rather similar positions of bands. The FTIR spectroscopic of raw *Peganum harmala-L* analyses indicated free and hydrogen bonded OH groups (3401 cm$^{-1}$) and carboxylic or phenolic stretching band (2925 cm$^{-1}$). The peak in 1631 cm$^{-1}$ was ascribed to C=O stretching of carboxylic acid and the peak in 1363 cm$^{-1}$ band occurred from N–H bend. The FTIR spectra show that the peaks at 722.00, 874.61, 1163.62, 1363.81, 1464.36, 1554.95, 1631.83, 1745.94, 2925.77, 3009.26, and 3401.13 cm$^{-1}$ in raw adsorbent shifted to 720, 1164, 1238, 1373, 1457, 1550, 1645, 1744, 2360, 2926, 3007, and 3457 cm$^{-1}$ in treated adsorbent, respectively. Decrease and increase of the peaks show that treating and modifying occurred.

*3.2. Effect of pH on the Adsorption.* The pH of the system is very important on the adsorption capacity due to its influence on the surface properties of the adsorbent and ionization/dissociation of the adsorbate molecule. The pH effect (from 2.0 to 10.0) on the Ni (II) adsorption by TPHS is shown in Figure 3(a). As the initial pH value increased from 2.0 to 8.0, the removal of Ni (II) by TPHS increased from 65.96% to 89.79%. Further, increasing the pH value from 8.0 to 10.0 did not significantly enhance the removal of Ni (II) (from 89.79% to 93.17%). The main reason for these phenomena could be explained as follows. There were a lot of $H_3O^+$ ions that competed with Ni (II) for the exchange sites in the adsorbent when the initial pH value was low [19], thus was prevented the removal of $Ni^{2+}$. When there was an increase in the initial pH value, the concentration of $H_3O^+$ ions decreased, and more Ni (II) could react with the released effective exchange sites. As can be seen in Figure 3(a), the highest nickel ions uptake was observed at pH 10 which was 93% due to precipitation of Ni ions from 8 to 10. Thus, the

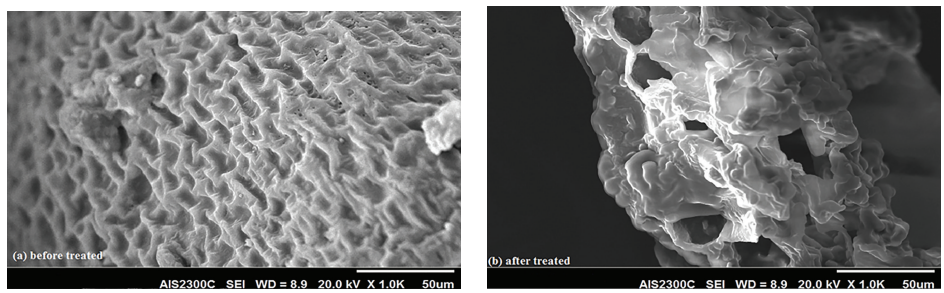


(a) (b)

Figure 1: SEM images of *Peganum harmala-L* (a) before and (b) after being treated.

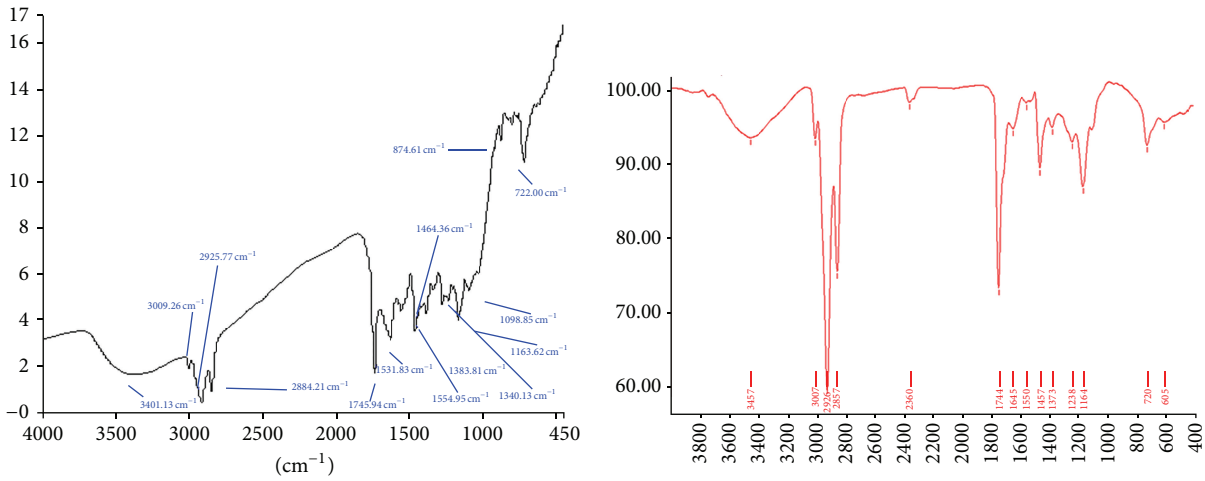


(a) (b)

Figure 2: FTIR spectra of *Peganum harmala-L* (a) before and (b) after being treated.

optimized pH was 7, and the rest of the experiments were considered at this optimized pH.

The mechanism the biosorption of Ni (II) onto TPHS can be represented by the following expressions:

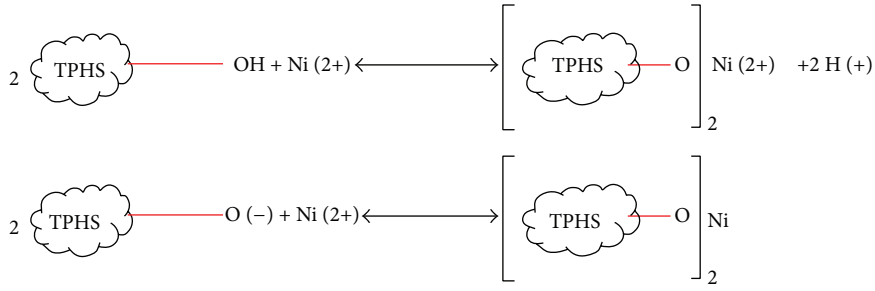


(13)

*3.3. Effect of TPHS Dosage on the Adsorption.* The effect of TPHS dosage on nickel adsorption was studied in the range of 1.0–15.0 mg. The result of nickel removal at various TPHS dosages is presented in Figure 3(b). The amount of adsorbent significantly influences the amount of Ni (II) adsorption. By increasing the amount of adsorbent, the surface area and adsorption capacity of adsorbent increased. It was found that by increasing the amount of adsorbents from 1.0 to 7.0 mg, the removal percentage increased rapidly from 86.75 to 95.31% and further addition has not significantly affected the Ni ions

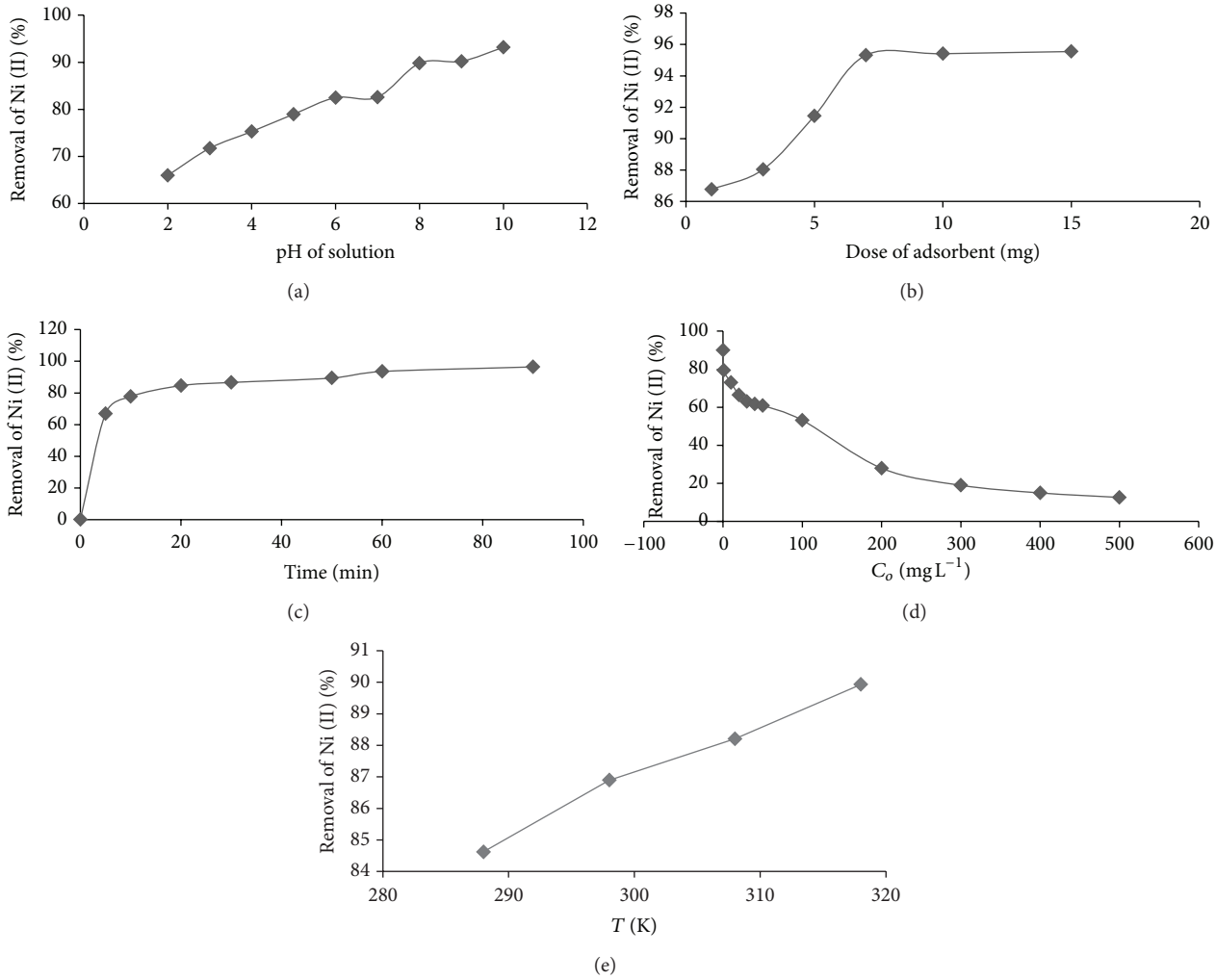


Figure 3: (a) Effect of pH, (b) effect of MPHS dosage, (c) effect of contact time, (d) effect of initial concentration, and (e) effect of temperature on removal of Ni ion by TPHS.

removal percentage. Thus, 7.0 mg of TPHS was fixed as the optimum dosage, and the rest of the studies were carried out at this optimum adsorbent pre-treated.

*3.4. Effect of Contact Time on the Adsorption.* Equilibrium time is one of the most important parameters in the design of economical wastewater treatment systems. The effect of contact time on the removal of Ni (II) by the TPHS at $C_o$ 100 mg/L for $M$ = 7 mg showed rapid adsorption of Ni (II) in the first 20 min and, thereafter, the adsorption rate decreased gradually and the adsorption reached equilibrium in about 90 min as shown in Figure 3(c). It may also be observed from Figure 3(c) that more than 84.62% of ion adsorption is taking place within the contact time of 20 min and increases gradually thereafter. The rapid adsorption at the initial contact time was due to the availability of more active surface of the adsorbents, which leads to fast adsorption of the ion from the solution. The later slow rate of ion adsorption probably occurred due to the less availability of active site onto the surface of adsorbent as well as the slow diffusion of the solute into the adsorbent pore [20]. Hence, 90 min contact time was chosen as the optimized time for the adsorbent for latter experiments.

*3.5. Effect of Initial Metal Concentration on the Adsorption.* The effect of $C_o$ on the removal of Ni ions by TPHS is shown in Figure 3(d). When the $C_o$ increased from 0.1 to 500 mg/L, the amount of Ni ions adsorbed per unit mass of TPHS ($q_e$) increased from 0.12 to 89.69 mg g$^{-1}$, whereas the percentage of Ni ions removal decreased from 90.0% to 12.55% with the increase in $C_o$. The percentage removal of the ions decreased slowly in the concentration range of 0.1–50.0 mg L$^{-1}$ but reduced rapidly from 50.0 to 500.0 mg/L. Ion removal is highly concentration dependent at higher concentrations. This can be explained by the fact that the adsorbent has a limited number of active sites that become saturated above a certain concentration. At low ion concentrations, the ratio of surface active sites to the total ions in the solution is high, and hence all ions may interact with the active functional groups on the surface of the adsorbent and be removed from

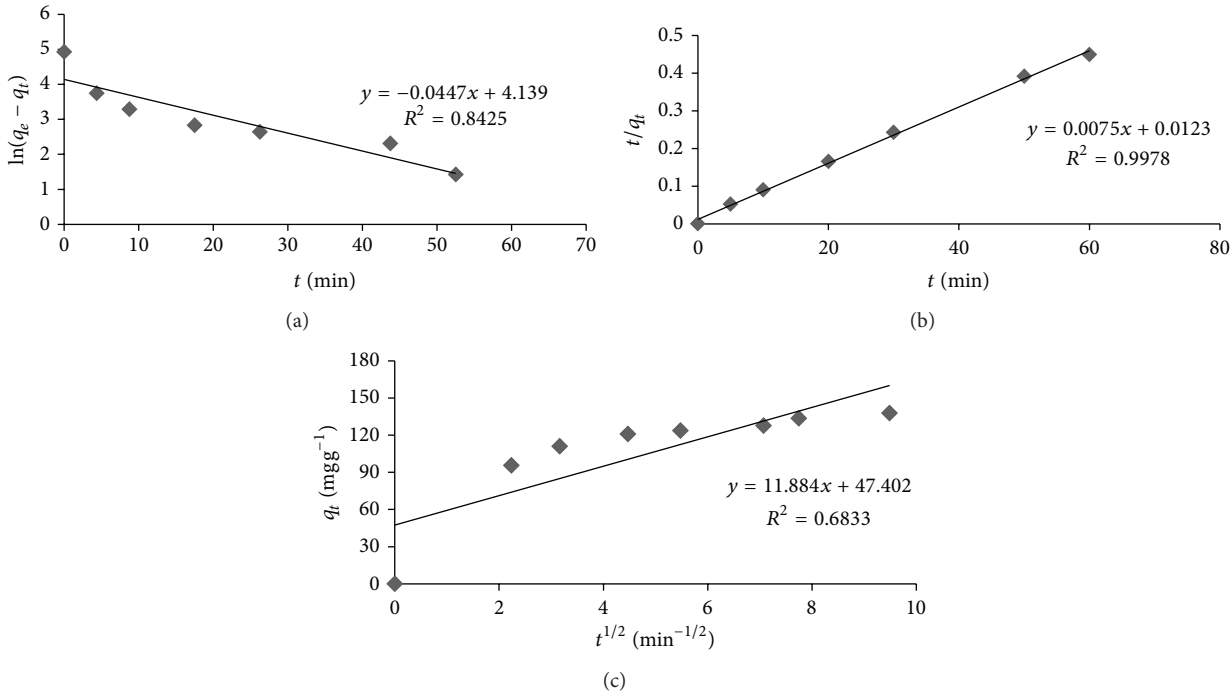


Figure 4: (a) Plot of the pseudo-first-order model. (b) Plot of the pseudo-second-order model. (c) Plot of the intraparticle model of Ni (II) on TPHS.

solution. However, with increasing ion concentrations, the number of active adsorption sites is not enough [21].

*3.6. Effect of Temperature on the Adsorption.* The temperature can affect the adsorption rate. The effect of temperature on nickel adsorption was investigated in the range of 288–318 K. The result of nickel removal at is presented in Figure 3(e). By increasing temperature of solution, adsorption capacity increased. It was found that by increasing it from 288 to 318 K, the removal percentage increased from 84.62 to 89.93%.

*3.7. Kinetic Study.* In order to investigate the adsorption behavior of metal ions on adsorbent, the pseudo-first, pseudo-second order kinetic and intraparticle models were used. The fitted linear form of the pseudo-first and pseudo-second order model is shown in Figures 4(a) and 4(b). The values of adsorption rate constants such as $k_1$, $k_2$, and $q_e$ for the two kinetic models were calculated by the method described in Section 2.5. Table 1 shows these adsorption rate constants, with regression coefficients ($R^2$). Regarding the value of $R^2$ of the pseudo-second-order and the pseudo-first order one, the pseudo-second-order model is more appropriate. The kinetic experimental data have been predicted well with this model and the correlation coefficient value for experiment was more than 0.99. For $Ni^{2+}$, the $q_e$ value predicted from the second-order-model is much more comparable to the experimental $q_e$ value than that from the first-order-model.

The pseudo-first-order and pseudo-second-order models cannot identify the diffusion mechanism. To determine whether the intraparticle diffusion is the rate limiting step

Table 1: Kinetic constants for the adsorption of Ni ions on TPHS.

| Kinetic model | Parameters | TPHS |
|---|---|---|
| Pseudo-first-order | $q_e$ (cal) (mg/g) | 137.783 |
| | $q_e$ (exp) (mg/g) | 62.740 |
| | $K_1$ (1/min) | 0.044 |
| | $R^2$ | 0.842 |
| Pseudo-second-order | $q_e$ (cal) (mg/g) | 137.783 |
| | $q_e$ (exp) (mg/g) | 133.33 |
| | $K_2$ (g/mg·min) | 0.004 |
| | $R^2$ | 0.997 |
| Intraparticle mass transfer | $k_d$ (mg/g·min) | 11.884 |
| | $C$ (mg/g) | 47.402 |
| | $R^2$ | 0.683 |

Table 2: Isotherm constants for the adsorption of Ni ions on TPHS.

| Isotherm model | Parameters | TPHS |
|---|---|---|
| Langmuir isotherm | $q_m$ (mg/g) | 91.743 |
| | $K_L$ (L/mg) | 0.049 |
| | $R^2$ | 0.997 |
| Freundlich isotherm | $1/n$ | 0.620 |
| | $K_F$ (L/mg) | 1.836 |
| | $R^2$ | 0.942 |
| Temkin isotherm | $M_T$ (mg/g) | 9.872 |
| | $K_T$ (L/mg) | 7.690 |
| | $R^2$ | 0.810 |

Table 3: Thermodynamic constants for the adsorption of Ni ions on TPHS.

| Adsorbent | Maximum capacity (mg/g) | Optimum condition | References |
|---|---|---|---|
| Pomegranate peel | 51.80 | $T = 25^{\circ}C$<br>pH = 5.5–6.5<br>adsorbent dosage = 10 g/L | Bhatnagar and Minocha [10] |
| *Litchi chinensis* seeds | 66.62 | $T = 25^{\circ}C$<br>pH = 7.5<br>adsorbent dosage = 1 g/L | Flores-Garnica et al. [22] |
| Acid-treated *Oedogonium hatei* | 44.24 | $T = 25^{\circ}C$<br>pH = 5.0<br>adsorbent dosage = 0.7 g/L | Gupta et al. [23] |
| *Moringa oleifera* bark | 26.84 | $T = 30^{\circ}C$<br>pH = 6.0<br>adsorbent dosage = 0.4 g/L | Reddy et al. [24] |
| *Saccharum bengalense* | 15.79 | $T = 60^{\circ}C$<br>pH = 5.0<br>adsorbent dosage = 10 g/L | Din and Mirza [25] |
| Modified *Moringa oleifera* leaves powder | 138.04 | $T = 20^{\circ}C$<br>pH = 6.0<br>adsorbent dosage = 10 g/L | Reddy et al. [26] |
| Treated *Peganum harmala-L* seeds | 91.74 | $T = 25^{\circ}C$<br>pH = 7.0<br>adsorbent dosage = 0.7 g/L | This study |

in the adsorption of Ni (II) onto TPHS, the intraparticle diffusion model proposed by Weber and Morris was used to analyze the kinetic results. The plot of $q_t$ versus $t^{1/2}$ for the adsorption of Ni (II) onto TPHS is shown in Figure 4(c). As can be seen from Figure 4(c), the intercept of the line does not pass through the origin and the correlation coefficients ($R^2$) are less than 0.99 suggesting that two or more steps are involved in the nickel adsorption onto the prepared adsorbent. The deviation of straight line in Weber and Morris model may be due to difference in the rate of mass transfer in the initial and final stages of adsorption [10].

*3.8. Equilibrium Study.* Isotherms state the particular correlation between the content of Ni (II) adsorbed onto TPHS surface in given empirical conditions and the equilibrium concentration of Ni (II) in the liquid phase. Linear plot of the Langmuir isotherm of Ni (II) ion adsorption on TPHS is shown in Figure 5(a).

The calculated constants for the described models in Section 2.6 and correlation coefficients are given in Table 2. As can be seen from Table 2, the Langmuir isotherm shows an inadequate fit of experimental data. The maximum adsorption capacity of TPHS ($q_m$) and the adsorption energy coefficient $K_L$ calculated from the slope and the intercept of the linear plot were 91.74 mg/g and 0.049 L mg$^{-1}$ at temperature 25°C, respectively. Figure 5(b) shows the variation of separation factor ($R_L$) with initial Ni ion concentration. The results that the $R_L$ values were in the range of 0-1 (from 0.9951 to 0.0392) indicate that the adsorption of Ni ion by adsorbent is favorable. The $R_L$ value is approaching zero with the increase of $C_o$ means that the adsorption of Ni ion onto TPHS is less favorable at high initial Ni ion concentration.

Linear plots of Freundlich and Temkin isotherm of Ni (II) ion adsorption on TPHS were shown in Figures 5(c) and 5(d). The Freundlich and Temkin constants calculated from the linear equations were summarized in Table 2. The value of $1/n$ was in the range of 0-1 that shows favorable adsorption on adsorbent. The correlation coefficient of the Freundlich and Temkin values was lower than the Langmuir value. The suitability of Langmuir data for interpretation of experimental suggests that ions adsorption is limited to monolayer coverage [27]. From linear regression of the data points, the $R^2$ value of 0.81 for Ni (II) is rather low which indicates that biosorption of Ni (II) did not follow the Temkin isotherm closely.

*3.9. Comparison of Adsorption Capacity with Different Adsorbents Reported in the Literature.* The maximum monolayer adsorption capacities of TPHS adsorbent for the removal of Ni (II) were compared with those of other adsorbents reported in the literature and the values are shown in Table 3. It is clear from Table 3 that the adsorption capacity of TPHS adsorbent was greater than the previously reported.

*3.10. Thermodynamics Study.* Results were shown in Table 4 and Figure 6. The negative values of $\Delta G$ changes found confirm the spontaneous nature of the process and the values of $\Delta G$ increase by increasing of temperature that show the feasibility of adsorption of Ni (II) adsorption onto TPHS. The values of $\Delta H^{\circ}$ and $\Delta S^{\circ}$ calculated from the equation are given as 11.979 kJ/mol and 0.058 kJ/mol K, respectively. The positive enthalpy change value of Ni (II) adsorption on TPHS indicate that the adsorption is an endothermic process. The positive entropy change value for Ni (II) adsorption on TPHS is due to

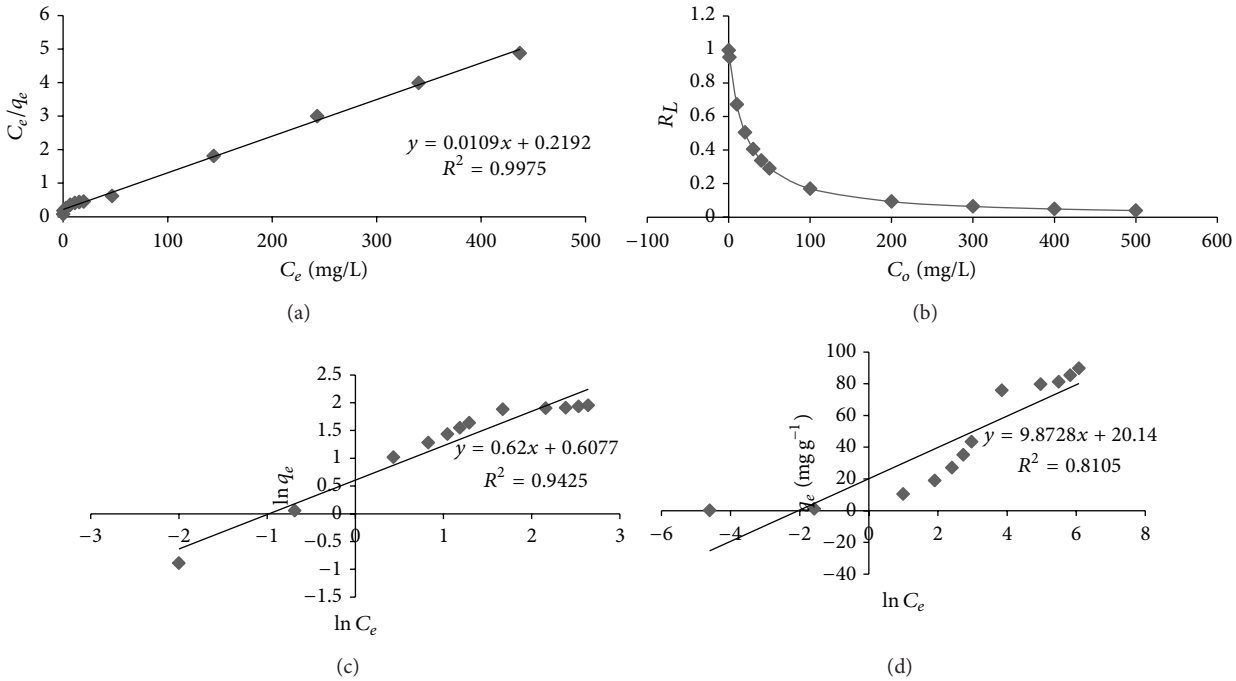


Figure 5: (a) The Langmuir isotherm plot. (b) Variation of separation factor ($R_L$) as a function of initial Ni (II) ion concentration. (c) The Freundlich isotherm plot and (d) Temkin isotherm plot of Ni (II) ion on TPHS.

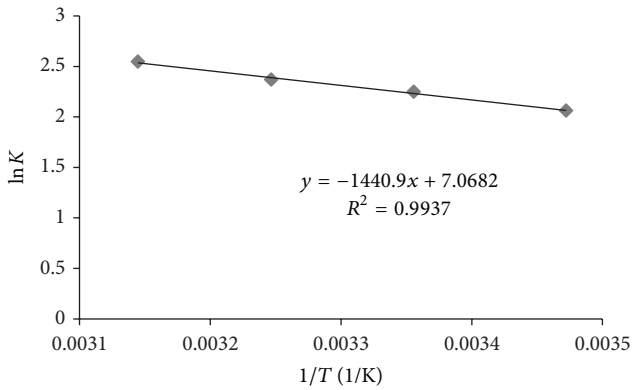


Figure 6: Plot of the ln $K$ versus temperature ($1/T$) for TPHS.

Table 4: Thermodynamic constants for the adsorption of Ni ions on TPHS.

| $T$ (K) | $\Delta G^\circ$ (kJ/mol) | $\Delta H^\circ$ (kJ/mol) | $\Delta S^\circ$ (kJ/mol·K) |
|---|---|---|---|
| 288 | −4.936 | 11.979 | 0.0587 |
| 298 | −5.570 | | |
| 308 | −6.065 | | |
| 318 | −6.731 | | |

increasing randomness at the solid-solution interface during the adsorption process [28]. According to Huang et al. [29], $\Delta H^\circ$ value physisorption was smaller than 40 kJ/mol and this value for our study shows that the adsorption of Ni (II) onto TPHS was a physisorption process ($\Delta H^\circ = 11.979$ kj·mol$^{-1}$).

## 4. Conclusions

This study demonstrated that treated adsorbent which was developed from *Peganum harmala-L* seeds could be used as an effective adsorbent for the removal of Ni (II) from aqueous solution. The equilibrium time for adsorption of Ni (II) from aqueous solutions was achieved within 90 min of contact time. Kinetics studies showed better applicability for pseudo-second-order model for this adsorbent. The isotherm study indicated that adsorption data correlated well with the Langmuir isotherm model. The maximum monolayer adsorption capacities for the removal of Ni (II) using TPHS adsorbent was found 91.74 mg/g. Thermodynamic constants were also evaluated using equilibrium constants changing with temperature. The negative values of $\Delta G^\circ$ suggested that the adsorption was spontaneous in nature. Finally, it can be concluded that the use of TPHS as an adsorbent may be an alternative to more costly materials, such as ion-exchange resins and carbon nanotubes, for the treatment of liquid wastes containing toxic Ni (II) metal ion.

## Conflict of Interests

The authors declare that there is no conflict of interests regarding the publication of this paper.

## Acknowledgment

The authors are thankful to the Faculty of Science, Department of Chemistry, Islamic Azad University, Arak Branch, Iran.

## References


[1] C. Lu, C. Liu, and G. P. Rao, "Comparisons of sorbent cost for the removal of $Ni^{2+}$ from aqueous solution by carbon nanotubes and granular activated carbon," *Journal of Hazardous Materials*, vol. 151, no. 1, pp. 239–246, 2008.

[2] V. K. Gupta and A. Nayak, "Cadmium removal and recovery from aqueous solutions by novel adsorbents prepared from orange peel and $Fe_2O_3$ nanoparticles," *Chemical Engineering Journal*, vol. 180, pp. 81–90, 2012.

[3] X. Huang, N.-Y. Gao, and Q.-L. Zhang, "Thermodynamics and kinetics of cadmium adsorption onto oxidized granular activated carbon," *Journal of Environmental Sciences*, vol. 19, no. 11, pp. 1287–1292, 2007.

[4] M. R. Panuccio, A. Sorgonà, M. Rizzo, and G. Cacco, "Cadmium adsorption on vermiculite, zeolite and pumice: batch experimental studies," *Journal of Environmental Management*, vol. 90, no. 1, pp. 364–374, 2009.

[5] J. Hizal and R. Apak, "Modeling of cadmium(II) adsorption on kaolinite-based clays in the absence and presence of humic acid," *Applied Clay Science*, vol. 32, no. 3-4, pp. 232–244, 2006.

[6] J. T. Bamgbose, S. Adewuyi, O. Bamgbose, and A. A. Adetoye, "Adsorption kinetics of cadmium and lead by chitosan," *African Journal of Biotechnology*, vol. 9, no. 17, pp. 2560–2565, 2010.

[7] E. W. Shin, K. G. Karthikeyan, and M. A. Tshabalala, "Adsorption mechanism of cadmium on juniper bark and wood," *Bioresource Technology*, vol. 98, no. 3, pp. 588–594, 2007.

[8] S. Kocaoba, "Adsorption of Cd(II), Cr(III) and Mn(II) on natural sepiolite," *Desalination*, vol. 244, no. 1–3, pp. 24–30, 2009.

[9] H. Kalavathy, B. Karthik, and L. R. Miranda, "Removal and recovery of Ni and Zn from aqueous solution using activated carbon from *Hevea brasiliensis*: batch and column studies," *Colloids and Surfaces B: Biointerfaces*, vol. 78, no. 2, pp. 291–302, 2010.

[10] A. Bhatnagar and A. K. Minocha, "Biosorption optimization of nickel removal from water using *Punica granatum* peel waste," *Colloids and Surfaces B: Biointerfaces*, vol. 76, no. 2, pp. 544–548, 2010.

[11] S. Lagergren, "Zur theorie der sogenannten adsorption gelöster stoffe, Kungliga Svenska Vetenskapsakademiens," *Handlingar*, vol. 24, no. 4, pp. 1–39, 1898.

[12] Y. S. Ho and G. McKay, "Sorption of dye from aqueous solution by peat," *Chemical Engineering Journal*, vol. 70, no. 2, pp. 115–124, 1998.

[13] W. J. Weber and J. C. Morris, "Kinetics of adsorption on carbon from solution," *Journal of the Sanitary Engineering Division*, vol. 89, no. 2, pp. 31–59, 1963.

[14] I. Langmuir, "The adsorption of gases on plane surfaces of glass, mica and platinum," *The Journal of the American Chemical Society*, vol. 40, no. 9, pp. 1361–1403, 1918.

[15] K. R. Hall, L. C. Eagleton, A. Acrivos, and T. Vermeulen, "Pore- and solid-diffusion kinetics in fixed-bed adsorption under constant-pattern conditions," *Industrial and Engineering Chemistry Fundamentals*, vol. 5, no. 2, pp. 212–223, 1966.

[16] H. M. F. Freundlich, "Über die adsorption in lösungen," *Ber Zeitschrift für Physikalische Chemie A*, vol. 57, pp. 385–470, 1906.

[17] M. Temkin, "Die gasadsorption und der nernstsche wärmesatz," *Acta Physicochimica URSS*, vol. 1, no. 1, pp. 36–52, 1934.

[18] M. Ghasemi, Mu. Naushad, N. Ghasemi, and Y. Khosravi-fard, "A novel agricultural waste based adsorbent for the removal of Pb(II) from aqueous solution: kinetics, equilibrium and thermodynamic studies," *Journal of Industrial and Engineering Chemistry*, vol. 20, no. 2, pp. 454–461, 2014.

[19] K. Zhu, H. Fu, J. Zhang, X. Lv, J. Tang, and X. Xu, "Studies on removal of $NH_4^+$-N from aqueous solution by using the activated carbons derived from rice husk," *Biomass and Bioenergy*, vol. 43, pp. 18–25, 2012.

[20] M. Ghaedi, H. Hossainian, M. Montazerozohori et al., "A novel acorn based adsorbent for the removal of brilliant green," *Desalination*, vol. 281, no. 1, pp. 226–233, 2011.

[21] L. Wang, "Application of activated carbon derived from "waste" bamboo culms for the adsorption of azo disperse dye: kinetic, equilibrium and thermodynamic studies," *Journal of Environmental Management*, vol. 102, pp. 79–87, 2012.

[22] J. G. Flores-Garnica, L. Morales-Barrera, G. Pineda-Camacho, and E. Cristiani-Urbina, "Biosorption of Ni(II) from aqueous solutions by *Litchi chinensis* seeds," *Bioresource Technology*, vol. 136, pp. 635–643, 2013.

[23] V. K. Gupta, A. Rastogi, and A. Nayak, "Biosorption of nickel onto treated alga (*Oedogonium hatei*): application of isotherm and kinetic models," *Journal of Colloid and Interface Science*, vol. 342, no. 2, pp. 533–539, 2010.

[24] D. H. K. Reddy, D. K. V. Ramana, K. Seshaiah, and A. V. R. Reddy, "Biosorption of Ni(II) from aqueous phase by *Moringa oleifera* bark, a low cost biosorbent," *Desalination*, vol. 268, no. 1–3, pp. 150–157, 2011.

[25] M. I. Din and M. L. Mirza, "Biosorption potentials of a novel green biosorbent *Saccharum bengalense* containing cellulose as carbohydrate polymer for removal of Ni(II) ions from aqueous solutions," *International Journal of Biological Macromolecules*, vol. 54, pp. 99–108, 2013.

[26] D. H. K. Reddy, K. Seshaiah, A. V. R. Reddy, and S. M. Lee, "Optimization of Cd(II), Cu(II) and Ni(II) biosorption by chemically modified *Moringa oleifera* leaves powder," *Carbohydrate Polymers*, vol. 88, no. 3, pp. 1077–1086, 2012.

[27] M. Ghaedi, M. N. Biyareh, S. N. Kokhdan et al., "Comparison of the efficiency of palladium and silver nanoparticles loaded on activated carbon and zinc oxide nanorods loaded on activated carbon as new adsorbents for removal of Congo red from aqueous solution: kinetic and isotherm study," *Materials Science and Engineering C*, vol. 32, no. 4, pp. 725–734, 2012.

[28] Q. Li, L. Chai, and W. Qin, "Cadmium(II) adsorption on esterified spent grain: equilibrium modeling and possible mechanisms," *Chemical Engineering Journal*, vol. 197, pp. 173–180, 2012.

[29] L. Huang, Y. Sun, T. Yang, and L. Li, "Adsorption behavior of Ni(II) on lotus stalks derived active carbon by phosphoric acid activation," *Desalination*, vol. 268, no. 1–3, pp. 12–19, 2011.